

Report on Numerical Performance to “An efficient augmented Lagrangian method for dynamic optimal transport on surfaces based on second-order cone programming”

Liang Chen*

Youyicun Lin†

Yuxuan Zhou‡

June 11, 2025

Abstract

This document presents snapshots of the distribution evolutions for all numerical experiments from the paper “An efficient augmented Lagrangian method for dynamic optimal transport on surfaces based on second-order cone programming” [1]. The results are reproducible via the open-source software `DOTs-SOCP` accompanying the paper, which is publicly available on GitHub¹.

1 Numerical examples

The examples that we tested are listed below ([1, Section 6.2]).

Example 1. *The transportation problem on the spiral surface given in Figure 1, discretized with $|V| = 9686$.*



Figure 1: From left to right: the initial distribution ρ_0 , the terminal distribution ρ_1 , and the discrete surface mesh. The darker color means a larger density value.

Example 2. *The transportation problem on the spiral surface given in Figure 2, a spherical surface from which three distinct rectangular regions have been removed. Moreover, we require that the transport process must bypass these “holes”. The surface is discretized with $|V| = 17463$.*

Example 3. *The transportation problem on the surface given in Figure 3 from [2], discretized with $|V| = 1515$. We also test a similar problem with different distributions, discretized with vertex $|V| = 6054$.*

Example 4. *The transportation problem on the surface² given in Figure 4, discretized with $|V| = 5047$ or $|V| = 34834$.*

*School of Mathematics, Hunan University, Changsha, 410082, China (chl@hnu.edu.cn).

†School of Mathematics, Hunan University, Changsha, 410082, China (linyouyicun@hnu.edu.cn).

‡Department of Mathematics, Southern University of Science and Technology, Shenzhen, 518055, China (zhouyx8@mail.sustech.edu.cn).

¹<https://github.com/chlhn/DOTs-SOCP>

²From The Stanford 3D Scanning Repository (<https://graphics.stanford.edu/data/3Dscanrep/>).



Figure 2: From left to right: the initial distribution ρ_0 concentrated on the bottom part, the terminal distribution ρ_1 concentrated on the top part, and the discrete surface mesh with $|V| = 17463$.



Figure 3: In each row, from left to right: the initial distribution ρ_0 , the terminal distribution ρ_1 , and the discrete surface mesh ($|V| = 1515$ for the top row and $|V| = 6054$ for the bottom row). The darker color means a larger density value.

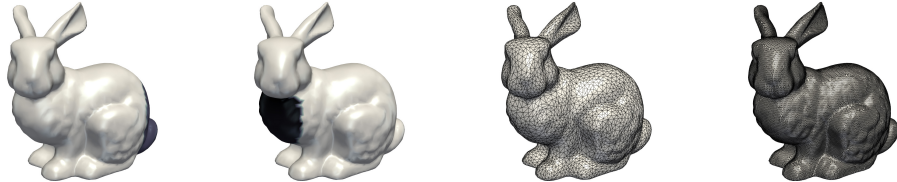


Figure 4: From left to right: the initial distribution ρ_0 concentrated at the tail, the terminal distribution ρ_1 concentrated at the chest, the discrete surface mesh with $|V| = 5047$, and the finer discrete surface mesh with $|V| = 34834$.

Example 5. *The transportation problem on the surface given in Figure 5 (comes from [2]), discretized with $|V| = 3772$ or $|V| = 15082$. Note that the meshes are not evenly distributed.*

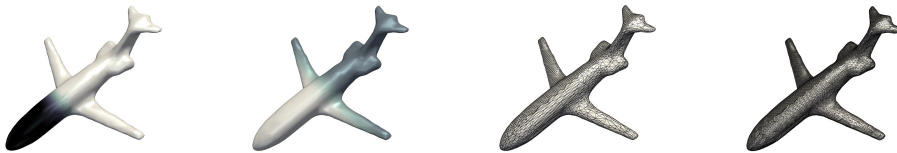


Figure 5: From left to right: the initial distribution ρ_0 , the terminal distribution ρ_1 , the discrete surface mesh with $|V| = 3772$, and the finer discrete surface mesh with $|V| = 15082$. The darker color means a larger density value.

Example 6. *The transportation problem on the surface given in Figure 6 (comes from [2]), discretized with $|V| = 5002$ or $|V| = 20002$.*

Example 7. *The transportation problem on the surface (of a hill) given in Figure 7, discretized with $|V| = 10000$.*

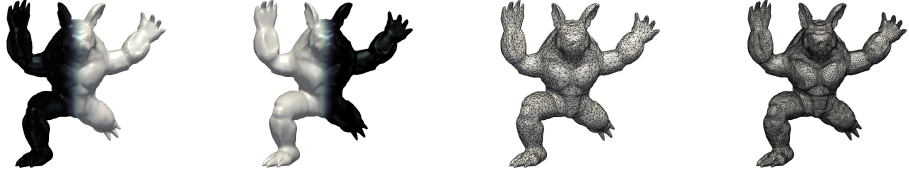


Figure 6: From left to right: the initial distribution ρ_0 , the terminal distribution ρ_1 , the discrete surface mesh with $|V| = 5002$, and the finer discrete surface mesh with $|V| = 20002$.



Figure 7: From left to right: the initial distribution ρ_0 , the terminal distribution ρ_1 , and the discrete surface mesh.

Example 8. *The transportation problem on the surface of a trefoil knot given in Figure 8, discretized with $|V| = 4096$.*



Figure 8: From left to right: the initial distribution ρ_0 , the terminal distribution ρ_1 , and the discrete surface mesh. The darker color means a larger density value.

Example 9. *The transportation problem on the surface of a cinquefoil knot given in Figure 9, discretized with $|V| = 4096$.*



Figure 9: From left to right: the initial distribution ρ_0 , the terminal distribution ρ_1 , and the discrete surface mesh. The darker color means a larger density value.

2 Snapshots of density evolutions

This part presents the snapshots of the density evolution for Examples 1 to 9 obtained by the software.

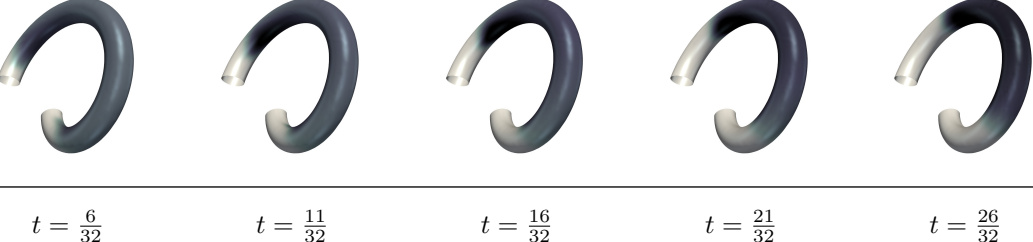


Figure 10: Snapshots of intermediate distribution evolution (from $t = \frac{6}{32}$ to $t = \frac{26}{32}$) for Example 1 obtained by software ($\text{Tol} = 10^{-4}$). The initial distribution ($t = 0$) and terminal distribution ($t = 1$) are shown in Figure 1.

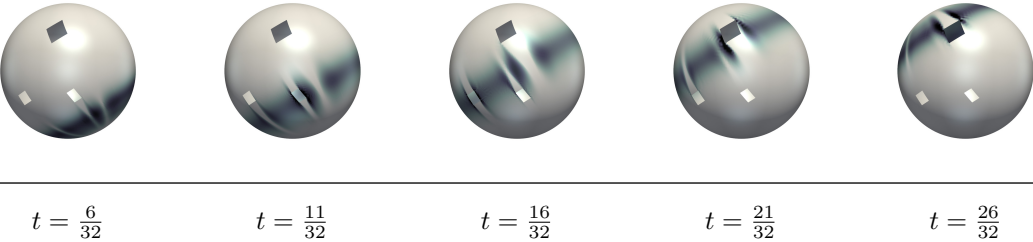


Figure 11: Snapshots of intermediate distribution evolution (from $t = \frac{6}{32}$ to $t = \frac{26}{32}$) for Example 2 obtained by software ($\text{Tol} = 10^{-4}$). The initial distribution ($t = 0$) and terminal distribution ($t = 1$) are shown in Figure 2.

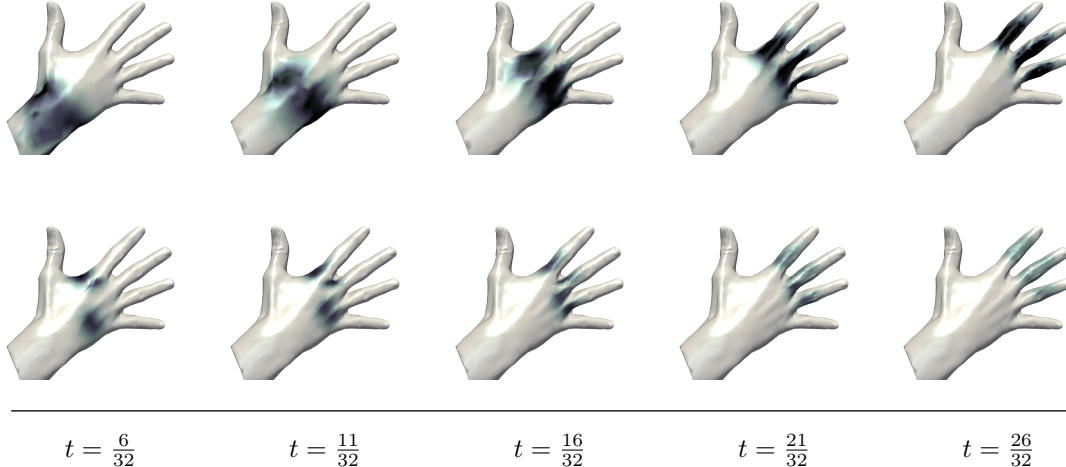


Figure 12: Snapshots of intermediate distribution evolution (from $t = \frac{6}{32}$ to $t = \frac{26}{32}$) for Example 3 obtained by software ($\text{Tol} = 10^{-4}$). The initial distribution ($t = 0$) and terminal distribution ($t = 1$) are shown in Figure 3.

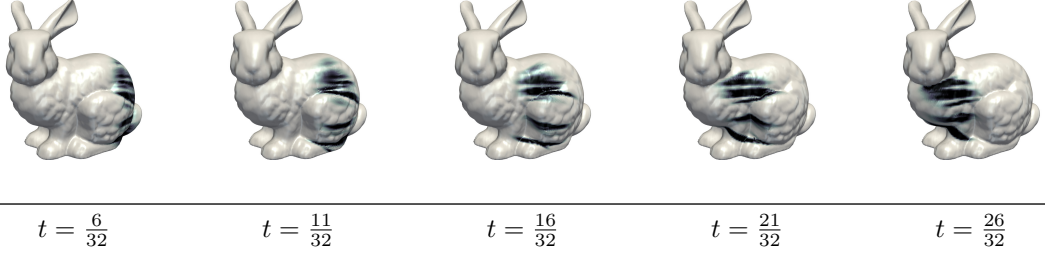


Figure 13: Snapshots of intermediate distribution evolution (from $t = \frac{6}{32}$ to $t = \frac{26}{32}$) for Example 4 $|V| = 34834$ obtained by software ($\text{Tol} = 10^{-4}$). The initial distribution ($t = 0$) and terminal distribution ($t = 1$) are shown in Figure 4.

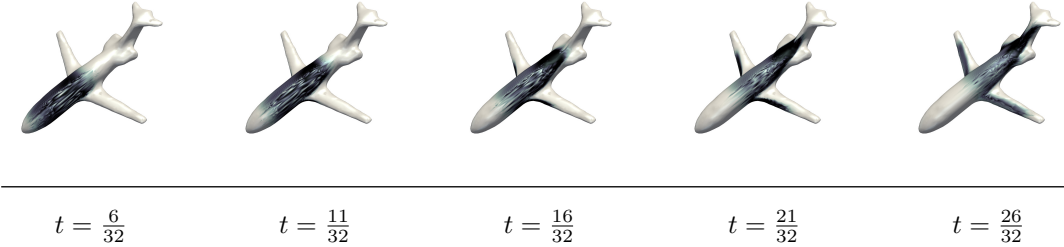


Figure 14: Snapshots of intermediate distribution evolution (from $t = \frac{6}{32}$ to $t = \frac{26}{32}$) for Example 5 with $|V| = 15082$ obtained by software ($\text{Tol} = 10^{-4}$). The initial distribution ($t = 0$) and terminal distribution ($t = 1$) are shown in Figure 5.

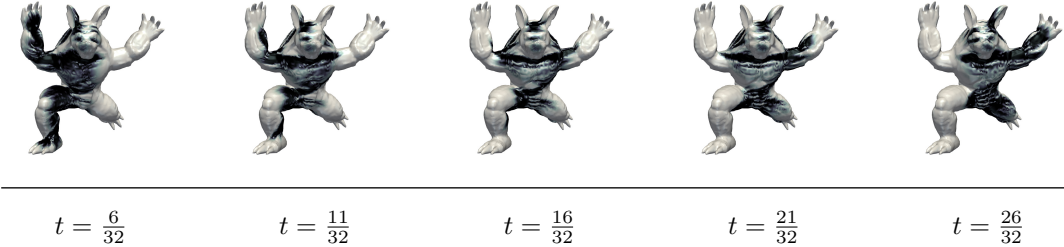


Figure 15: Snapshots of intermediate distribution evolution (from $t = \frac{6}{32}$ to $t = \frac{26}{32}$) for Example 6 obtained by software ($\text{Tol} = 10^{-4}$). The initial distribution ($t = 0$) and terminal distribution ($t = 1$) are shown in Figure 6.

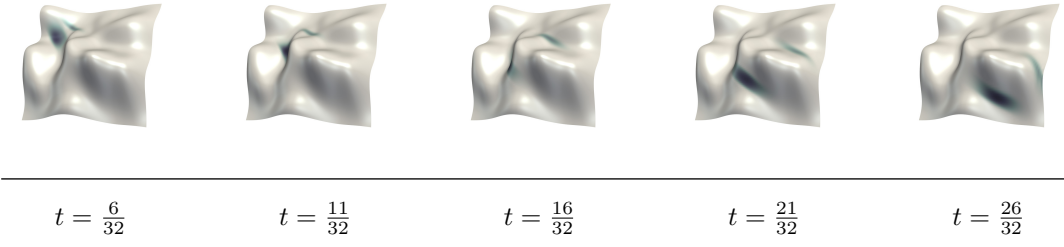


Figure 16: Snapshots of intermediate distribution evolution (from $t = \frac{6}{32}$ to $t = \frac{26}{32}$) for Example 7 obtained by software ($\text{Tol} = 10^{-4}$). The initial distribution ($t = 0$) and terminal distribution ($t = 1$) are shown in Figure 7.



$$t = \frac{6}{32}$$

$$t = \frac{11}{32}$$

$$t = \frac{16}{32}$$

$$t = \frac{21}{32}$$

$$t = \frac{26}{32}$$

Figure 17: Snapshots of intermediate distribution evolution (from $t = \frac{6}{32}$ to $t = \frac{26}{32}$) for Example 8 obtained by software ($\text{Tol} = 10^{-4}$). The initial distribution ($t = 0$) and terminal distribution ($t = 1$) are shown in Figure 8.



$$t = \frac{6}{32}$$

$$t = \frac{11}{32}$$

$$t = \frac{16}{32}$$

$$t = \frac{21}{32}$$

$$t = \frac{26}{32}$$

Figure 18: Snapshots of intermediate distribution evolution (from $t = \frac{6}{32}$ to $t = \frac{26}{32}$) for Example 9 obtained by software ($\text{Tol} = 10^{-4}$). The initial distribution ($t = 0$) and terminal distribution ($t = 1$) are shown in Figure 9.

3 Comparison under different congestion factors

This part presents the density evolutions for Examples 7 to 9, computed via the software based on the inexact semi-proximal ALM for solving [1, Eq. (52)] with a varying congestion parameter θ . The snapshots in Figures 19 to 21 confirm that a larger θ leads to a significant reduction in congestion.

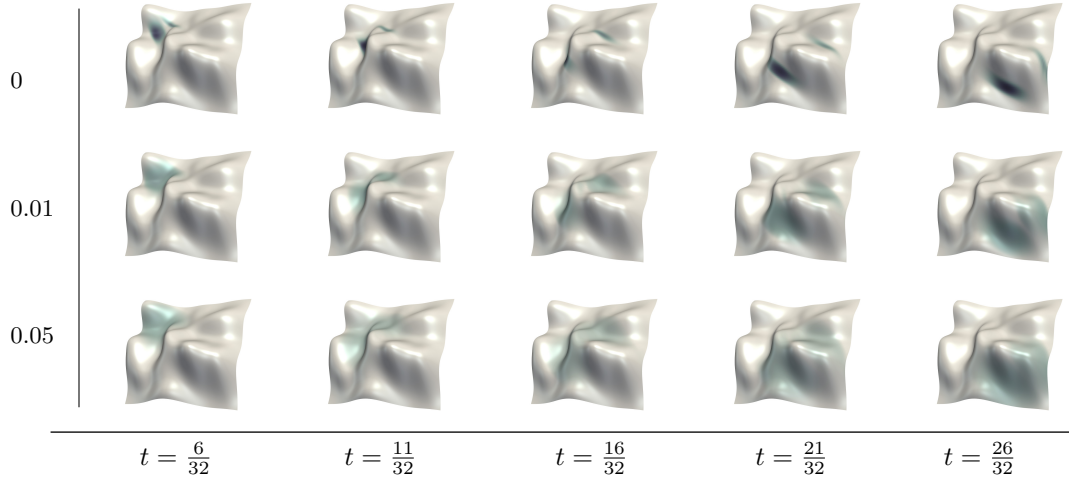


Figure 19: Snapshots of intermediate distribution evolution (from $t = \frac{6}{32}$ to $t = \frac{26}{32}$) for Example 7 obtained by software ($\text{Tol} = 10^{-4}$) with different regularization parameter θ ($= 0, 0.01, \text{ and } 0.05$). The initial distribution ($t = 0$) and terminal distribution ($t = 1$) are shown in Figure 7.

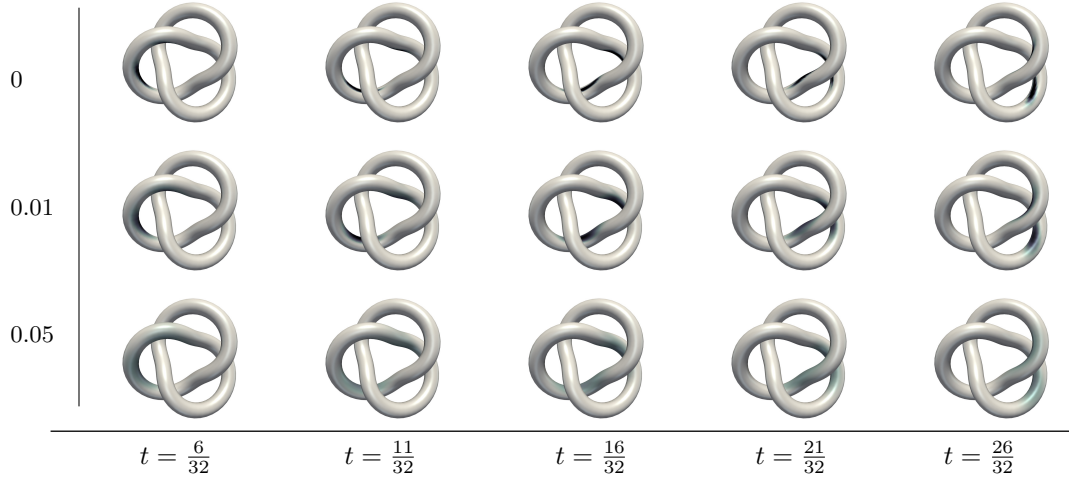


Figure 20: Snapshots of intermediate distribution evolution (from $t = \frac{6}{32}$ to $t = \frac{26}{32}$) for Example 8 obtained by software ($\text{Tol} = 10^{-4}$) with different regularization parameter θ ($= 0, 0.01, \text{ and } 0.05$). The initial distribution ($t = 0$) and terminal distribution ($t = 1$) are shown in Figure 8.

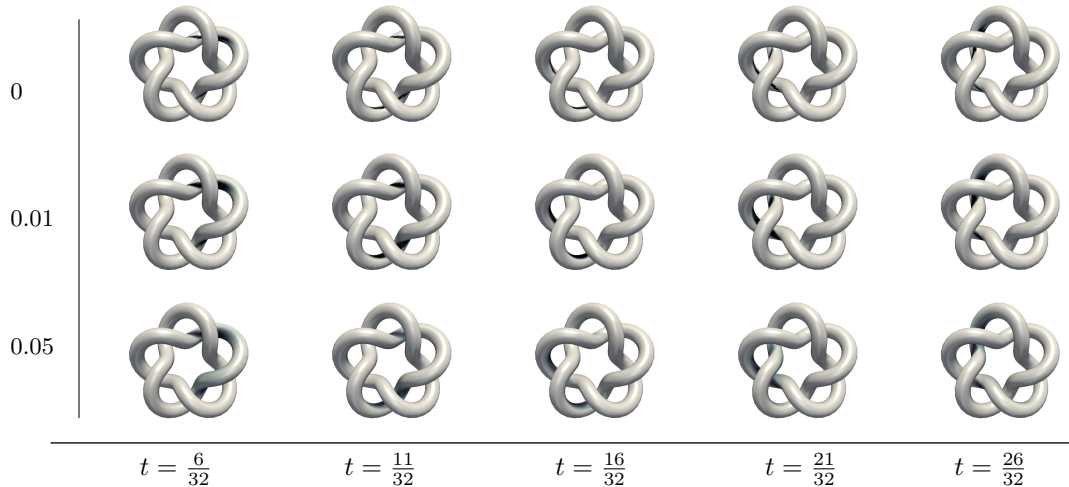


Figure 21: Snapshots of intermediate distribution evolution (from $t = \frac{6}{32}$ to $t = \frac{26}{32}$) for Example 9 obtained by software ($\text{Tol} = 10^{-4}$) with different regularization parameter θ ($= 0, 0.01$, and 0.05). The initial distribution ($t = 0$) and terminal distribution ($t = 1$) are shown in Figure 9.

References

- [1] L. Chen, Y.Y.C. Lin, and Y.X. Zhou, An efficient augmented Lagrangian method for dynamic optimal transport on surfaces based on second-order cone programming, arXiv preprint [arXiv:2506.08988](https://arxiv.org/abs/2506.08988) (2025).
- [2] H. Lavenant, S. Claici, E. Chine, and J. Solomon, Dynamical optimal transport on discrete surfaces, ACM Trans. Graph., 37 (2018), pp. 1-16.